Journal of Catalysis 259 (2008) 269–275

Contents lists available at ScienceDirect

Journal of Catalysis

www.elsevier.com/locate/jcat

Effect of extra-framework gallium on the structure of iron species in Fe/ZSM-5

Haian Xia [a,b], Keqiang Sun [a], Fengtao Fan [a,b], Keju Sun [a,b], Weiguang Su [a,b], Zhaochi Feng [a], Pinliang Ying [a], Can Li [a,*]

[a] State Key Laboratory of Catalysis, Dalian Institute of Chemical Physics, Chinese Academy of Sciences, 457 Zhongshan Road, Dalian 116023, China
[b] Graduate Schools of the Chinese Academy of Sciences, Beijing 100039, China

ARTICLE INFO

Article history:
Received 14 July 2008
Revised 31 August 2008
Accepted 2 September 2008
Available online 27 September 2008

Keywords:
Raman spectroscopy
N_2O decomposition
Transient response
Extra-framework Ga
Isolated
Bi-nuclear
Oligo-nuclear

ABSTRACT

A series of Fe/Ga-ZSM-5 catalysts with different Ga contents were prepared by solid-state ion exchange method. Ultraviolet and visible Raman spectroscopy, ultraviolet–visible diffuse reflectance spectroscopy, H_2-temperature-programmed reduction, and N_2O decomposition at 523 K were used to investigate the effect of extra-framework Ga on the nature of the Fe species in Fe/Ga-ZSM-5 catalysts. Introducing extra-framework Ga and high-temperature treatment can significantly affect the distribution even the nature of the Fe species in Fe/Ga-ZSM-5. For the high-temperature treated catalysts, the presence of extra-framework Ga remarkably increases the amount of the Fe(II) sites and the activity of direct N_2O decomposition, suggesting that extra-framework Ga can promote the formation of the active sites for N_2O decomposition. The possible interpretation of the beneficial role of extra-framework Ga is that extra-framework Ga facilitates the reduction of bi- and oligo-nuclear Fe(III) sites to form the Fe(II) sites and interacts with the Fe sites with low nuclearity to form a mixed Fe–Ga–O phase for the high-temperature treated catalysts.

1. Introduction

Fe/ZSM-5 catalysts are widely studied because of their unique properties in direct catalytic N_2O decomposition [1–4], selective catalytic reduction of NO_x with hydrocarbons or ammonia [5–9], and oxidative dehydrogenation of alkanes [10]. More interestingly, it was found that Fe/ZSM-5 catalysts show high activity and selectivity in the hydroxylation of benzene to phenol and methane to methanol at room temperature with N_2O as the oxidant [11,12]. An analogy of these catalytic behaviors between Fe/ZSM-5 and some enzymes such as soluble methane mono-oxygenase (sMMO) suggests that there might be similarity in the structure of active sites between them [11,12].

Different Fe species can be present as mono-, bi-nuclear or oligo-nuclear cationic species, neutral iron oxide species with a varying degree of agglomeration, mixed oxide phases combining Fe and Al, and bulk iron oxides on the external surface of the zeolite [12–32]. The exact preparation and pretreatment methods strongly affect the distribution even nature of the iron species in Fe/ZSM-5. High-temperature treatment or steaming increases catalytic activity in N_2O decomposition and benzene oxidation substantially [12,15–17,21]. A large number of studies have attempted to assign the active site as N_2O decomposition. Extra-framework isolated Fe ions [33,34], bi-nuclear Fe cluster [12,20,35,36], and oligo-nuclear Fe clusters [17,19] have been supposed to be the active sites for direct N_2O decomposition. Dubkov et al. have found an evidence that the activity is related to the formation of a specific iron site denoted α-sites [12]. Furthermore, the heteroatom (e.g., Al, Ga, B) may also play an important role in the formation of the active Fe sites [14,16–18,20,27,37]. Our previous results have shown that the introduction of extra-framework Al by post-synthesized method and high-temperature treatment can increase the amount of α-sites and the activity of N_2O decomposition on Fe/ZSM-5 catalysts [18]. The formation of Fe–O–Al mixed oxides has been proposed as the active sites [14–17,20]. It was reported that Fe/Ga-ZSM-5 catalyst exhibits higher activity than Fe/Al-ZSM-5 in the hydroxylation of benzene using N_2O as an oxidant [37]. However, the role of extra-framework Ga species played in the formation of the active sites remains to be investigated. The detection of the various Fe species is a very challenging task due to the heterogeneity of the iron species and the low concentrations of the active iron species in the micropores of ZSM-5.

The present study aims to investigate the effect of extra-framework Ga on the structure of the Fe species and the activity of direct N_2O decomposition, and to study the role of extra-framework Ga played in the formation of the active Fe species. For this purpose, a series of catalysts were prepared via post-synthesized method and characterized by ultraviolet (UV) and visible Raman spectroscopy, UV–visible diffuse reflectance spectroscopy, and H_2-temperature-programmed reduction (H_2-TPR). It is found that the addition of extra-framework Ga can remarkably change the distribution and nature of the iron species, and favor

* Corresponding author. Fax: +86 411 84694447.
E-mail address: canli@dicp.ac.cn (C. Li).
URL: http://www.canli.dicp.ac.cn (C. Li).

0021-9517/$ – see front matter
doi:10.1016/j.jcat.2008.09.001

Table 1
The chemical component of the catalysts treated in He at 1173 K and the amount of the Fe(II) sites determined by different methods.

Catalyst	Fe (wt%)	Ga (wt%)	Fe(II) sites (10^{19} sites/g)[a]	α-sites (10^{19} sites/g)[b]
Fe-ZSM-5-HT	1.02	0	2.5	1.9
Fe/Ga-ZSM-5(0.74)-HT	1.0	0.74	3.8	2.2
Fe/Ga-ZSM-5(1.61)-HT	1.02	1.61	5.0	2.8

[a] Determined by N_2O decomposition at 523 K.
[b] Determined by O_2-TPD followed by N_2O decomposition at 523 K.

the formation of the Fe(II) sites and increase the activity of N_2O decomposition on Fe/Ga-ZSM-5 catalysts.

2. Experimental

2.1. Preparation of the catalysts

Fe/ZSM-5 catalysts were prepared by solid-state ion exchange method, and the details have been described elsewhere [19,20]. The Fe/Ga-ZSM-5 was also prepared by solid-state ion exchange method. Firstly, the exchange of H-ZSM-5 with $FeCl_3$ was performed at 593 K for 2 h, and then cooled to room temperature in a glove box. Subsequently, the sample was mixed with a desired amount of $GaCl_3$, followed by removal from the glove box, and then the mixture was heated in Ar flow from room temperature to 473 K at a rate of 8 K/min with an isothermal period at final temperature for 2 h. Finally, the solid was treated in a flow of 0.5 vol% water in Ar from room temperature to 473 K to hydrolysis Fe–Cl and Ga–Cl bonds. After the hydrolysis, the samples were calcined in O_2 at 823 K for 2 h to obtain Fe/ZSM-5-C without extra-framework Ga and Fe/Ga-ZSM-5(x)-C with extra-framework Ga, where x denotes extra-framework Ga loading, and C refers to the calcination in O_2 at 823 K. A portion of calcined Fe/Ga-ZSM-5-C was further treated in He flow at 1173 K for 2 h to obtain Fe/Ga-ZSM-5-HT, where HT denotes a pretreatment in He at 1173 K.

2.2. Characterization

The chemical compositions of the catalysts were determined by inductively coupled plasma-atomic emission spectrometry (ICP-AES). The chemical components of the catalysts are listed in Table 1.

X-ray powder diffraction patterns were collected in Rigaku Miniflex diffractometer with Cu$K\alpha$ radiation source. Data collected in the 2θ range of 5–60° at a scan rate of 5°/min. The results show that bulk Fe oxides and bulk Ga oxides are not observed (not shown).

UV–visible diffuse reflectance spectra were taken on a JASCO V-550 spectrometer under ambient conditions. $BaSO_4$ was used as a reference material.

UV Raman spectra were recorded on a home-built UV Raman spectroscopy with spectral resolution of 2 cm^{-1}. The lased line of a He–Cd laser was used as an exciting source with an output of 25 mW. About 50 mg of catalyst sample was pressed into a wafer and placed in an in situ cell contained inlet and outlet gas connections. To obtain the Raman spectra in the dehydrated conditions and decrease the fluorescence interference, Fe/ZSM-5-C and Fe/Ga-ZSM-5(x)-C ($x = 0.74$ and 1.61) were calcined in O_2 at 823 K for 1 h, while Fe/ZSM-5-HT and Fe/Ga-ZSM-5(x)-HT ($x = 0.74$ and 1.61) were firstly treated in O_2 at 823 K for 1 h followed by a pretreatment in He at 1173 K for 1 h. After these treatments, the samples were cooled to room temperature to record the spectrum.

Visible Raman spectra were collected on a Spex 1877D Raman spectrograph with a laser line at 532 nm. The catalyst sample was pressed into a thin disk and fixed in a quartz cell. The details of the treatment processes are described as follows: treating the sample at 823 K in flow O_2 for 1 h to remove organic remnants, followed by a pretreatment in flowing He at 1173 K for 1 h; then, introducing N_2O/He (5%) to the catalyst at 523 K. After each treatment, the quartz cell was quickly sealed and cooled to room temperature to record Raman spectrum.

H_2-TPR experiments were carried out with a H_2/Ar (5.0%) flow of 25 ml/min from 300 to 1250 K with a ramp of 8 K/min. Before each H_2-TPR run, Fe/ZSM-5-C and Fe/Ga-ZSM-5(x)-C ($x = 0.74$ and 1.61) were pretreated in O_2 at 823 K for 1 h, while Fe/ZSM-5-HT and Fe/Ga-ZSM-5(x)-HT ($x = 0.74$ and 1.61) were pretreated in Ar at 1173 K for 1 h. The H_2 consumption was determined by a thermal conductivity detector (TCD).

Two methods were applied to determine the concentration of the Fe(II) sites. The first one is similar to the transient-response technique adopted by Kiwi-Minisker et al. [26]. The reaction effluent is continuously monitored after a step change from He flow to N_2O/He (5.0%) flow: the decomposition of N_2O will lead to gaseous N_2 concomitant with the deposition of an equal amount of surface oxygen species [12,26]. The concentration of the Fe(II) sites was estimated by integral of the amount of released N_2 based on the assumption that one oxygen atom is deposited per the Fe(II) sites [26]. It was reported that the O_2-temperature-programmed desorption (O_2-TPD) method can be used to determine the amount of the active oxygen species [26,38]. So, a complementary method was used to determine the amount of active oxygen species via O_2-TPD method following N_2O decomposition at 523 K. Typically, a 50 mg of catalyst sample was used to determine the concentration of the Fe(II) sites in these catalysts. Prior to each run, Fe/ZSM-5-C and Fe/Ga-ZSM-5(x)-C ($x = 0.74$ and 1.61) were pretreated in O_2 at 823 K for 1 h, while Fe/ZSM-5-HT and Fe/Ga-ZSM-5(x)-HT ($x = 0.74$ and 1.61) were pretreated at 1173 K for 1 h and then cooled to 523 K in He flow. Subsequently, The concentration of N_2O was quickly changed from 0 to 5.0 vol%.

2.3. Activity measurement

A single-pass plug-flow quartz reactor with an inner diameter of 4 mm was used for direct N_2O decomposition. A 50 mg catalyst sample was retained between two quartz wool plugs. Fe/ZSM-5-C and Fe/Ga-ZSM-5(x)-C ($x = 0.74$ and 1.61) were pretreated at 823 K in O_2 for 1 h, while Fe/ZSM-5-HT and Fe/Ga-ZSM-5(x)-HT ($x = 0.74$ and 1.61) were firstly treated at 823 K in O_2 for 1 h, followed by a pretreatment at 1173 K in He for 1 h. During steady-state catalytic measurements, the concentration of N_2O was 5.0 vol% and the gas hourly space velocity was kept at 24000 ml/g h. A well-calibrated on-line mass spectrometer (GAM 200; Pfeiffer vacuum) was used for quantification of gaseous products.

3. Results

3.1. The concentration of Fe(II) sites in Fe/ZSM-5 and Fe/Ga-ZSM-5 catalysts

Fig. 1A shows responses after a step change from He flow to N_2O/He (5.0 vol%) flow on Fe/ZSM-5-HT at 523 K. The evolution of N_2 is detected only, suggesting that only the reaction $N_2O + (\ )_{Fe} = N_2 + (O)_{Fe}$ occurs. The concentration of the Fe(II) sites available for the surface atomic oxygen species was estimated from the amount of released N_2. As shown in Table 1, the amount of the Fe(II) sites increases with increasing extra-framework Ga content. For Fe/ZSM-5-HT and Fe/Ga-ZSM-5(x)-HT ($x = 0.74$ and 1.61), the amount of the Fe(II) sites is 2.5×10^{19}, 3.8×10^{19}, and 5.0×10^{19} sites/(g catalyst), corresponding to an Fe(II)/Fe ratio of 0.23, 0.35, and 0.45, respectively. A blank experiment on Ga/ZSM-5 shows that the activity of solely extra-framework Ga is negligible. Similar

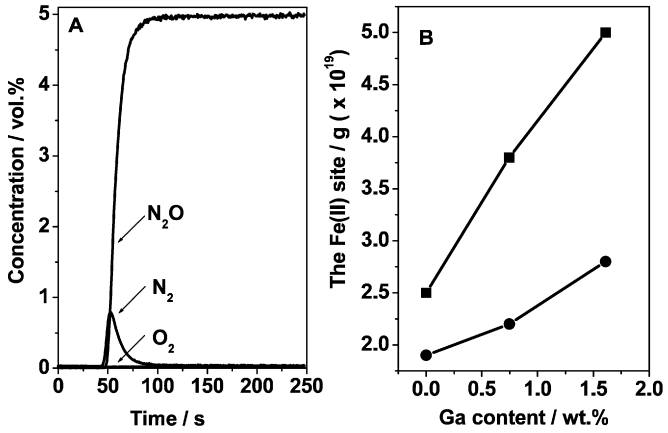

Fig. 1. (A) Responses after a step change from He flow to N_2O/He (5.0%) flow at 523 K on Fe-ZSM-5-HT. (B) The dependence of the amount of the Fe(II) sites and α-sites on extra-framework Ga content: (■) the Fe(II) sites determined by N_2O decomposition at 523 K, and (●) the Fe(II) sites determined by O_2-TPD method following N_2O decomposition at 523 K.

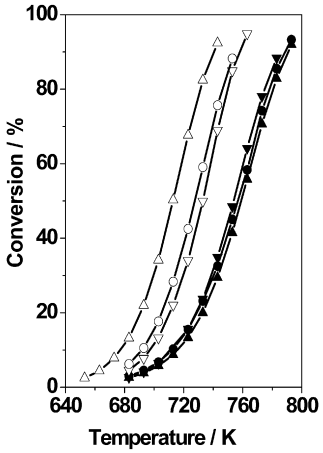

Fig. 2. N_2O conversion versus the reaction temperature over the catalysts calcined in O_2 at 823 K and treated in He at 1173 K: (▼) Fe/ZSM-5-C, (●) Fe/Ga-ZSM-5(0.74)-C, (▲) Fe/Ga-ZSM-5(1.61)-C, (▽) Fe/ZSM-5-HT, (○) Fe/Ga-ZSM-5(0.74)-HT, and (△) Fe/Ga-ZSM-5(1.61)-HT. Reaction conditions: N_2O/He (5.0%), GHSV = 24,000 h^{-1}.

experiments for Fe/ZSM-5-C and Fe/Ga-ZSM-5(x)-C ($x = 0.74$ and 1.61) catalysts showed that no N_2 was observed upon exposure of these catalysts to N_2O at 523 K, indicating that high temperature treatment is prerequisite for the formation of the active sites for N_2O decomposition at low temperature.

The amount of the active oxygen species, i.e., so-called α-oxygen, was further determined by O_2-TPD method [26], immediately following the decomposition of N_2O on Fe/ZSM-5 at 523 K. Table 1 lists the amounts of the Fe(II) sites determined by O_2-TPD method for Fe/ZSM-5-HT and Fe/Ga-ZSM-5(x)-HT ($x = 0.74$ and 1.61). The amount of α-oxygen is 1.9×10^{19}, 2.2×10^{19}, and 2.8×10^{19} sites/(g catalyst), corresponding to an O/Fe ratio of 0.17, 0.20, and 0.25 for Fe/ZSM-5-HT and Fe/Ga-ZSM-5(x)-HT ($x = 0.74$ and 1.61), respectively. This suggests that only a portion of surface atomic oxygen species deposited by N_2O decomposition can be measured by O_2-TPD method. This is in accordance with the observations that only a portion of the surface oxygen species deposited by N_2O decomposition are active for CO oxidation [26] or $^{18}O_2$ isotopic exchange [4]. Fig. 1B shows the correlation of the amount of the Fe(II) sites determined by different methods with extra-framework Ga content. It can be seen that the amounts of the Fe(II) sites and α-sites increase with increasing extra-framework Ga content, suggesting that the presence of extra-framework Ga species can favor the formation of the Fe(II) sites and α-sites.

3.2. Steady-state N_2O decomposition on Fe/ZSM-5 and Fe/Ga-ZSM-5 catalysts

Fig. 2 shows the N_2O conversion versus the reaction temperature of N_2O decomposition under steady-state conditions. It can be seen that Fe/ZSM-5-HT and Fe/Ga-ZSM-5(x)-HT ($x = 0.74$ and 1.61) exhibit higher catalytic activities of N_2O decomposition than those of Fe/ZSM-5-C and Fe/Ga-ZSM-5(x)-C ($x = 0.74$ and 1.61). The activity of N_2O decomposition decreases with increasing extra-framework Ga content on the catalysts calcined in O_2 at 823 K, while the activity of N_2O decomposition increases with the increase of extra-framework Ga content on the catalysts treated in He at 1173 K. A blank experiment on Ga/ZSM-5 shows that the activity of N_2O decomposition is negligible, suggesting that the introduction of extra-framework Ga can significantly change the activity for Fe/Ga-ZSM-5 catalysts, namely the activity of Fe-containing sites of the catalysts.

Kinetic parameters for these catalysts have been calculated from Arrhenius plots under the assumption of first-order disappearance of N_2O [39]. Table 2 lists the apparent activation energies and the pre-exponential factors of N_2O decomposition for these catalysts. The apparent activation energy for Fe/ZSM-5-C is about 181 kJ/mol, whereas the apparent activation energy decreases to 169 and 166 kJ/mol for Fe/Ga-ZSM-5(0.74)-C and Fe/Ga-ZSM-5(1.61)-C, respectively. Accordingly, the pre-exponential factor decreases from 3.0×10^7 mol N_2O s^{-1} (mol Fe)$^{-1}$ (Pa N_2O)$^{-1}$ for Fe/ZSM-5-C to 2.7×10^6 mol N_2O s^{-1} (mol Fe)$^{-1}$ (Pa N_2O)$^{-1}$ for Fe/Ga-ZSM-5(1.61)-C. After the high-temperature treatment, the apparent activation energy increases to 197, 192, and 195 kJ/mol for Fe/ZSM-5-HT, Fe/Ga-ZSM-5(0.74)-HT, and Fe/Ga-ZSM-5(1.61)-HT, respectively. This result shows that the structure of the active sites for N_2O decomposition could be similar for the catalysts treated in He at 1173 K.

Table 2
Apparent activation energies and pre-exponential factors of N_2O decomposition on the catalysts calcined in O_2 at 823 K and treated in He at 1173 K.

Sample	Pretreatment conditions	E_a (kJ/mol)	A (mol N_2O/s mol Fe Pa N_2O)
Fe/ZSM-5-C	823 K/O_2	181	3.0×10^7
Fe/Ga-ZSM-5(0.74)-C	823 K/O_2	169	4.1×10^6
Fe/Ga-ZSM-5(1.61)-C	823 K/O_2	166	2.7×10^6
Fe-ZSM-5-HT	1173 K/Ar	197	1.0×10^9
Fe/Ga-ZSM-5(0.74)-HT	1173 K/Ar	192	9.4×10^8
Fe/Ga-ZSM-5(1.61)-HT	1173 K/Ar	195	1.9×10^9

3.3. UV–visible diffuse reflectance spectra of Fe/ZSM-5 and Fe/Ga-ZSM-5 catalysts

Fig. 3A displays the UV–visible diffuse reflectance spectra of Fe/ZSM-5-C and Fe/Ga-ZSM-5(x)-C ($x = 0.74$ and 1.61). The catalysts exhibit two intense bands at 243 and 340 nm, as well as a shoulder at 540 nm. The bands at 243 and 340 nm are attributed to oxygen-to-iron charge transfer transition of isolated Fe ions and oligo-nuclear Fe clusters [19,20,35], respectively. It should be noted that the bi-nuclear Fe clusters contribute to the absorbance band in the region of 300–400 nm [20,40,41]. As shown in Fig. 3A, the intensities of the band at 340 nm and a shoulder at 540 nm increase while that of the band at 243 nm decreases with increasing extra-framework Ga content. To quantify the different Fe species, the UV–visible spectra were deconvoluted into Gaussian sub-bands according to the method reported in the literature [42,43]. A rough estimation of the percentage of the different Fe species in the catalysts was obtained from the fraction of sub-bands with respect to

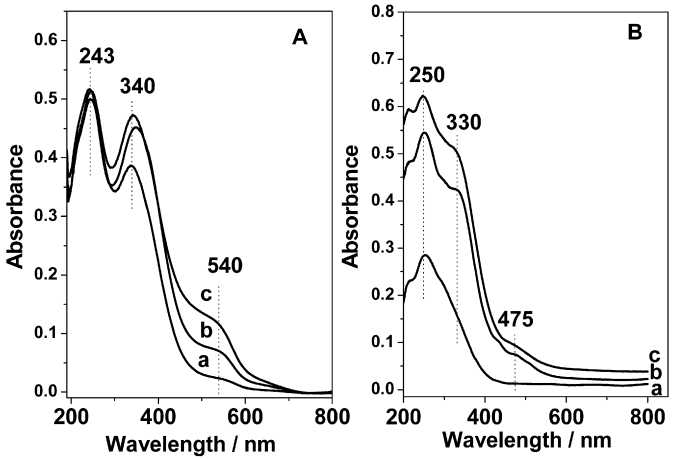

Fig. 3. UV–visible diffuse reflectance spectra of (A) the catalysts calcined in O_2 at 823 K: (a) Fe-ZSM-5-C, (b) Fe/Ga-ZSM-5(0.74)-C, and (c) Fe/Ga-ZSM-5(1.61)-C; and (B) the catalysts treated in He at 1173 K: (a) Fe/ZSM-5-HT, (b) Fe/Ga-ZSM-5(0.74)-HT, and (c) Fe/Ga-ZSM-5(1.61)-HT.

Table 3
Percentage of the area of sub-bands (I_1 at $\lambda < 300$ nm, I_2 at $300 < \lambda < 400$ nm, I_3 at $\lambda > 400$ nm) of UV–visible spectra of the catalysts (see Fig. 3) and corresponding iron percentage derived from total iron content (see Table 1).

Catalyst	Fe[a]		Fe[b]		Fe[c]	
	I_1 (%)	wt%	I_2 (%)	wt%	I_3 (%)	wt%
Fe-ZSM-5-C	61	0.62	30	0.31	9	0.09
Fe/Ga-ZSM-5(0.74)-C	52	0.52	35	0.35	13	0.13
Fe/Ga-ZSM-5(1.61)-C	45	0.46	37	0.38	18	0.18

[a] Isolated Fe ions in tetrahedral and octahedral.
[b] Oligo-nuclear Fe_xO_y clusters ($x \geqslant 2$).
[c] Bulk Fe oxides.

the total area of experimental spectrum multiplied with the total Fe content, as shown in Table 3. As can be seen, the percentage of isolated Fe ions decreases while those of oligo-nuclear Fe clusters and Fe oxide particles increases with increasing extra-framework Ga content, suggesting that extra-framework Ga leads to a agglomeration of isolated Fe ions into bi- and oligo-nuclear Fe clusters.

Fig. 3B displays the UV–visible diffuse reflectance spectra of Fe/ZSM-5-HT and Fe/Ga-ZSM-5(x)-HT ($x = 0.74$ and 1.61). The band at 243 nm becomes sharp and the intensities of the bands at 340 and 540 nm decrease substantially after the treatment in He at 1173 K. Two new bands at 330 and 475 nm are observed, which are tentatively ascribed to the oligo-nuclear Fe clusters and small Fe oxide particles [19], respectively. The intensity of the band at 330 nm increases with an increase in extra-framework Ga content, indicating that extra-framework Ga could change the nature of Fe species.

3.4. UV Raman spectra of Fe/ZSM-5 and Fe/Ga-ZSM-5 catalysts

Fig. 4A shows the UV Raman spectra of Fe/ZSM-5-C and Fe/Ga-ZSM-5(x)-C ($x = 0.74$ and 1.61) with the excitation line at 325 nm. Raman bands at 450, 880, 1005, and 1180 cm^{-1} are observed for Fe/ZSM-5-C and Fe/Ga-ZSM-5(x)-C ($x = 0.74$ and 1.61). Accordingly to our previous results [20], the bands at 450 and 880 cm^{-1} could be tentatively assigned to Fe–O–Fe symmetric and asymmetric stretching modes of a bi-nuclear cationic Fe species, respectively. The bi-nuclear cationic Fe species may be presented as such or be part of some Fe oxide phase of low Fe nuclearity. As can be seen, introducing extra-framework Ga remarkably increases in the intensities of the bands at 450 and 880 cm^{-1} and decreases in the intensities of the bands at 1005 and 1180 cm^{-1}. This suggests that extra-framework Ga results in a clustering of isolated Fe ions into

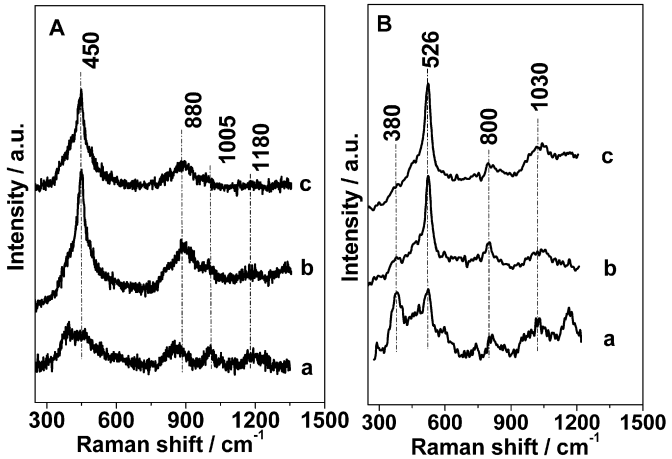

Fig. 4. UV Raman spectra with the excitation line at 325 nm of (A) the catalysts calcined in O_2 at 823 K: (a) Fe-ZSM-5-C, (b) Fe/Ga-ZSM-5(0.74)-C, and (c) Fe/Ga-ZSM-5(1.61)-C; and (B) the catalysts treated in He at 1173 K: (a) Fe/ZSM-5-HT, (b) Fe/Ga-ZSM-5(0.74)-HT, and (c) Fe/Ga-ZSM-5(1.61)-HT.

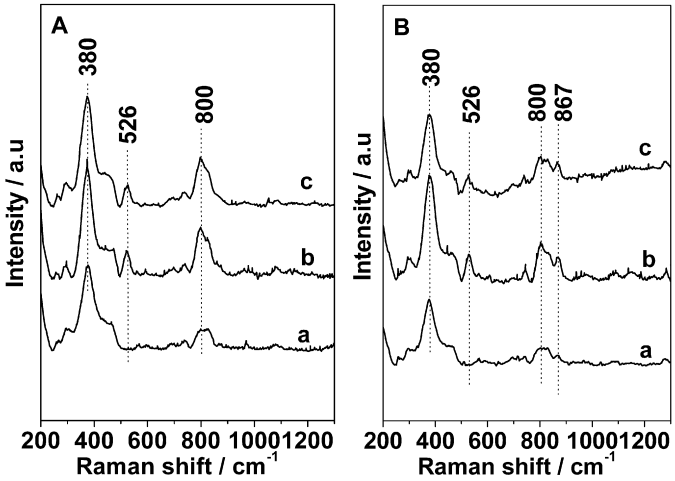

Fig. 5. Visible Raman spectra after different treatments: (A) the treatment in He at 1173 K and (B) N_2O decomposition at 523 K. The catalysts: (a) Fe/ZSM-5-HT, (b) Fe/Ga-ZSM-5(0.74)-HT, and (c) Fe/Ga-ZSM-5(1.61)-HT. The excitation line: 532 nm.

bi- and oligo-nuclear Fe clusters, in accordance with the UV–visible spectral results.

Fig. 4B shows the UV Raman spectra of Fe/ZSM-5-HT and Fe/Ga-ZSM-5(x)-HT ($x = 0.74$ and 1.61) with the excitation line at 325 nm. In addition to the Raman bands at 380 and 800 cm^{-1} characteristic of MFI structure of ZSM-5 [13,44], bands at 526 and 1030 cm^{-1} are also observed. This result suggests that the treatment in He at 1173 K significantly changes the structure of the Fe species. The bands at 526 and 1030 cm^{-1} are associated with the bi- and oligo-nuclear Fe clusters and isolated Fe ions [20], respectively. It can be seen that the intensity of the band at 526 cm^{-1} increases after the introduction of extra-framework Ga, implying that the incorporation of Ga results in an increase in the amount of the bi- and oligo-nuclear Fe sites on the catalysts treated in He in 1173 K.

3.5. Visible Raman spectra of Fe/ZSM-5 and Fe/Ga-ZSM-5 catalysts

Fig. 5A shows the visible Raman spectrum of the catalysts treated in He at 1173 K with the excitation line at 532 nm. Raman bands at 380, 526, and 800 cm^{-1} are observed. The intensity of the band at 526 cm^{-1} increases with increasing extra-framework Ga content, in agreement with the UV Raman spectral results (Fig. 4B).

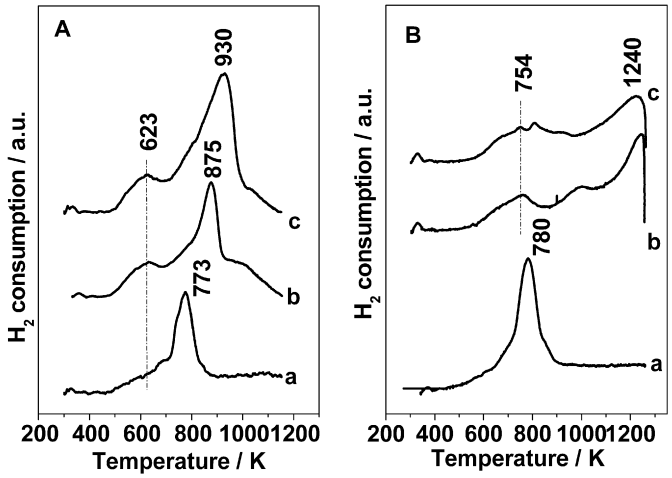

Fig. 6. H_2-TPR profiles of (A) the catalysts calcined in O_2 at 823 K: (a) Fe-ZSM-5-C, (b) Fe/Ga-ZSM-5(0.74)-C, and (c) Fe/Ga-ZSM-5(1.61)-C; and (B) the catalysts treated in He at 1173 K: (a) Fe/ZSM-5-HT, (b) Fe/Ga-ZSM-5(0.74)-HT, and (c) Fe/Ga-ZSM-5(1.61)-HT.

However, the intensity of the band at 526 cm^{-1} is weaker than that in the UV Raman spectra. This is due to resonance Raman enhanced effect, for the excitation line at 325 nm is close to the absorbance band at 330 nm (Fig. 3B). Fig. 5B shows the spectrum collected after exposing the high-temperature-pretreated Fe/ZSM-5 to N_2O at 523 K. A new peak at 867 cm^{-1} is observed, which has been assigned to the peroxide species bridged on the bi-nuclear Fe sites [35]. In order to compare the intensity of the band at 867 cm^{-1} among the catalysts treated in He at 1173 K, the band at 380 cm^{-1} was used as a inner criterion, and the deconvolution was performed for the bands in the 700–900 cm^{-1} region (not shown). It was found that the intensity ratios of the bands at 867 and 380 cm^{-1} increase with an increase in extra-framework Ga content (not shown), which is consistent with the transient response results that extra-framework Ga increases the amount of the surface oxygen species.

3.6. H_2-TPR of Fe/ZSM-5 and Fe/Ga-ZSM-5 catalysts

Fig. 6A presents the H_2-TPR profiles of Fe/ZSM-5-C and Fe/Ga-ZSM-5(x)-C ($x = 0.74$ and 1.61). The H_2-TPR profile of Fe/ZSM-5-C exhibits a reduction peak at 773 K and a small shoulder at 623 K. After the introduction of extra-framework Ga, the reduction peak shifts to 875 and 930 K for Fe/Ga-ZSM-5(0.74)-C and Fe/Ga-ZSM-5(1.61)-C, respectively. Moreover, the intensity of the peak at 623 K increases with increasing extra-framework Ga content. The peak at 623 K is due to bi-nuclear Fe clusters [5], and the reduction peaks at 875 and 930 K could be associated with Fe and Ga oxides.

Fig. 6B shows the H_2-TPR profiles of Fe/ZSM-5-HT and Fe/Ga-ZSM-5(x)-HT ($x = 0.74$ and 1.61). The H_2-TPR profile of Fe/ZSM-5-HT shows an intense peak at 780 K, while Fe/Ga-ZSM-5(x)-HT ($x = 0.74$ and 1.61) catalysts show two reduction peaks at 780 and 1240 K. The reduction peak at 780 K could be attributed to extra-framework Fe–O–Al species [45], while the peak at 1240 K could be associated with extra-framework Ga species.

4. Discussion

4.1. The effect of extra-framework Ga on the formation of Fe(II) sites

UV–visible, UV, and visible Raman spectral results show that the amount of isolated Fe ions decreases while that of bi- and oligo-nuclear Fe clusters increases with increasing extra-framework Ga content for the catalysts calcined in O_2 at 823 K. Upon the treatment in He at 1173 K, the bi-, and oligo-nuclear Fe species convert into the new bi-, and oligo-nuclear Fe species, which are characteristic of the new Raman band at 526 cm^{-1}. TPR results also show that the new reduction peak at 754 K is observed for Fe/Ga-ZSM-5(x) ($x = 0.74$ and 1.61) upon the treatment in He at 1173 K. Moreover, the reduction peak is shift from 780 K for Fe/ZSM-5-HT to 754 K for Fe/Ga-ZSM-5(x) ($x = 0.74$ and 1.61), suggesting that the nature of the Fe species is moderately changed.

Transient response results show that introducing extra-framework Ga increases the amounts of the Fe(II) sites and α-sites. It is found that only a portion of surface atomic oxygen species are so-called "α-oxygen," implying that the Fe(II) sites are heterogeneous and the active Fe(II) sites, i.e. α-sites, could be only a portion of the Fe(II) sites. It is found that the amount of isolated Fe ions decreases while the amount of the Fe sites increases with extra-framework Ga content for the catalysts calcined in O_2 at 823 K. The high-temperature treatment (1173 K/He) for the catalysts calcined in O_2 at 823 K further decreases the amount of isolated Fe ions due to the further agglomeration of isolated Fe ions into bi- and oligo-nuclear Fe clusters. Therefore, it seems most likely that the bi- and oligo-nuclear Fe sites contribute to the Fe(II) sites responsible for N_2O decomposition at low temperature.

It has been reported that the Fe^{2+} sites with low nuclearity are responsible for N_2O decomposition at low temperature [12,18,20,26,35]. High-temperature treatment can lead to the self-reduction of the Fe(III) sites to the Fe(II) sites [30]. Moreover, the self-reduction of bi- and oligo-nuclear Fe clusters are easier than that of isolated Fe ions upon high-temperature treatment based on thermodynamic data [30]. It was also reported that the presence of Al promotes the reduction of Fe(III) ions to Fe(II) ions, in particular for bi-nuclear and oligo-nuclear Fe clusters, on isomorphically substituted catalysts on the basis of Mössbauer spectroscopy [46]. Thus, the beneficial role of extra-framework Ga could be explained by one reason that extra-framework Ga increases the amount of bi- and oligo-nuclear Fe clusters and promotes the reduction of bi- and oligo-nuclear Fe clusters for the high-temperature treated catalysts (1173 K/He).

The other explanation for the beneficial role of extra-framework Ga is that extra-framework Ga could interact with the Fe sites with low nuclearity to form a mixed oxide. Our recent results have showed that the pivotal role of extra-framework Al species in the formation and stabilization of the bi-nuclear Fe sites [20]. More interestingly, it was also reported that the addition of extra-framework Ce/La can promote the activity of the selective catalytic reduction of NO with NH_3/iso-C_4H_{10} in Fe/ZSM-5, which is attributed to the reason that Fe and Ce/La could form the mixed oxides [47,48]. Thus, it is likely that extra-framework Ga interacts with the Fe sites with low nuclearity to form a mixed oxide.

4.2. The relation between structure and activity of direct N_2O decomposition

The conversion of N_2O decomposition and the apparent activation energy decrease with increasing extra-framework Ga content for the catalyst calcined in O_2 at 823 K. This could be explained by the reason that more clustering iron sites are benefited for N_2O decomposition [17,19,20]. Fig. 7 shows the correlation of the rate of N_2O decomposition at 773 K with the total amount of isolated Fe ions, bi-nuclear and oligo-nuclear Fe clusters estimated from the UV–visible spectra for the catalysts calcined in O_2 at 823 K. It can be seen that the rate of N_2O decomposition has good linear relationship with the total amount of isolated Fe ions, bi-nuclear and oligo-nuclear Fe clusters, indicating that isolated Fe ions, bi-nuclear and oligo-nuclear Fe clusters are the active sites for direct N_2O decomposition. Thus, the activity of direct N_2O decomposition slightly decreases with an increase in extra-framework Ga content

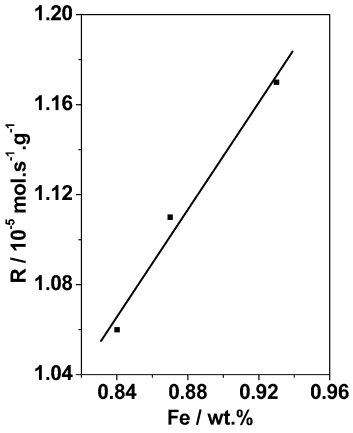

Fig. 7. The correlation of the rate of N_2O decomposition at 77 K with the total amount of isolated iron ions, bi-nuclear and oligo-nuclear iron clusters estimated from the UV–visible spectra on the catalysts calcined in O_2 at 823 K.

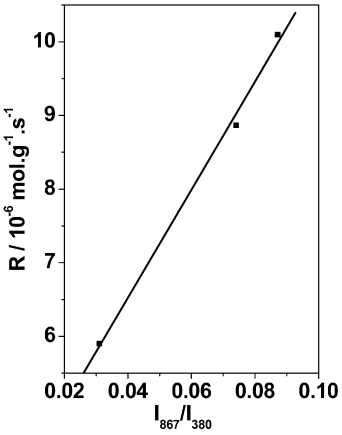

Fig. 8. The correlation of the rate of N_2O decomposition at 723 K with the intensity ratios of the bands at 867 and 380 cm^{-1} for the catalysts treated in He at 1173 K.

because the presence of extra-framework Ga increases the inactive bulk Fe oxide particles.

The treatment in He at 1173 K of the calcined catalysts remarkably increases the activity of direct N_2O decomposition. Moreover, the activity of direct N_2O decomposition increases with increasing extra-framework Ga content. The apparent activation energy lies around 190 kJ/mol, in line with literature values [3,19,20]. The apparent activation energy does not depend on the extra-framework Ga content which points to the uniform nature of the active sites. Fig. 8 depicts the correlation of the rate of N_2O decomposition at 723 K with the intensity ratios of the bands at 867 and 380 cm^{-1} for the catalysts treated in He at 1173 K. It can be seen that the rate of N_2O decomposition has good linear relationship with the intensity ratios of the band at 867 and 380 cm^{-1}, suggesting that the band at 867 cm^{-1} is related to the active sites for direct N_2O decomposition. It is thus proposed that the active sites for direct N_2O decomposition are the bi-nuclear Fe(II) sites since the band at 867 cm^{-1} is formed by N_2O decomposition on the bi-nuclear Fe(II) sites at 523 K. It is also possible that the bi-nuclear Fe(II) sites are stabilized by extra-framework Ga species on the high-temperature treated catalysts, i.e., extra-framework Fe–Ga–O species are possibly formed.

4.3. Comparison of the role of Al with Ga

The role of framework and extra-framework Al species in the formation of the active sites has been reported [14–18,37]. Hensen et al. have reported that the incorporation of Al species by post-synthesized method followed by steaming treatment can remarkably increase the activity of benzene oxidation to phenol. They proposed that an extra-framework Fe–Al–O species are responsible for benzene oxidation to phenol [14–17]. Our previous results have shown that the introduction of extra-framework Al increases the activity of N_2O decomposition on Fe/ZSM-5 catalysts [18]. In this work, it is found that the promotional role of extra-framework Ga species in the formation of the active sites is similar to that of extra-framework Al species reported in our previous work [18]. The incorporation of extra-framework Al or Ga into Fe/ZSM-5 remarkably promotes the activity of direct N_2O decomposition and the formation of the Fe(II) sites for the high-temperature treated catalysts. It was found that the high-temperature treated Ga/ZSM-5 catalysts do not exhibit the activity of N_2O direct decomposition. These results suggest that the synergetic effect of Ga could be existed for the high-temperature treated Fe/Ga-ZSM-5 catalysts. It is also possible that the high-temperature treatment can lead to the re-construction of the active sites to an extra-framework Fe–Ga–O mixed oxide. It should be noted that extra-framework B do not exhibit a promotional role in the formation of the Fe(II) sites determined by N_2O decomposition at 523 K on the high-temperature treated catalysts (not shown). A possible explanation is that the properties of B are different from those of Al and Ga, thus, B and Fe species could not form an extra-framework mixed oxide.

5. Conclusions

Introduction of extra-framework Ga species in Fe/ZSM-5 and the high-temperature treatment significantly change the distribution and even the nature of the Fe species. Introducing extra-framework Ga leads to an increase in the amount of the bi- and oligo-nuclear Fe clusters and bulk iron oxides for the calcined catalysts. After the high-temperature treatment of Fe/Ga-ZSM-5, the bi- and oligo-nuclear Fe clusters transform into a new bi- and oligo-nuclear Fe clusters stabilized by extra-framework Al or Ga species. Introduction of extra-framework Ga into Fe/ZSM-5 can remarkably increase the amount of the Fe(II) sites and the activity of direct N_2O decomposition, indicating that the interaction between extra-framework Fe and Ga is more efficient than solely Fe for the active sites and for direct N_2O decomposition. The possible explanation for the promotional role of extra-framework Ga could be that introducing extra-framework Ga facilitates the reduction of bi- and oligo-nuclear Fe(III) clusters to form the Fe(II) sites and interacts with the Fe(II) sites to form a mixed Fe–Ga–O phase on the high-temperature treated catalysts. It is shown that oligo-nuclear, perhaps bi-nuclear, iron sites appear most favorable for direct N_2O decomposition on the high-temperature treated catalysts.

Acknowledgments

This work was financially supported by the National Basic Research Program of China (grant No. 2005CB221407), Programme of the Strategic Scientific Alliances between China and the Netherlands (grant No. 2008DFB50130), the CAS-BP project, and the National Natural Science Foundation of China (grant Nos. 20673115, 20773118).

References

[1] E.M. El-Malki, R.A. van Santen, W.M.H. Sachtler, Microporous Mesoporous Mater. 35–36 (2000) 235.
[2] J. Pérez-Ramírez, F. Kapteijn, G. Mul, X.D. Xu, J.A. Moulijn, Catal. Today 76 (2002) 55.
[3] Q. Zhu, B.L. Mojet, R.A.J. Janssen, E.J.M. Hensen, J. van Grondelle, P. Magusin, R.A. van Santen, Catal. Lett. 81 (2002) 205.
[4] Q. Zhu, R.M. van Teeffelen, R.A. van Santen, E.J.M. Hensen, J. Catal. 221 (2004) 575.

[5] H.Y. Chen, W.M.H. Sachtler, Catal. Today 42 (1998) 73.
[6] K. Yamada, S. Kondo, K. Segawa, Microporous Mesoporous Mater. 35–36 (2000) 227.
[7] G. Centi, S. Perathoner, F. Vazzana, M. Marella, M. Tomaselli, M. Mantegazza, Adv. Environ. Res. 4 (2000) 325.
[8] Q. Sun, Z.X. Gao, H.Y. Chen, W.M.H. Sachtler, J. Catal. 201 (2001) 89.
[9] B. Wichterlová, Top. Catal. 28 (2004) 131.
[10] J. Pérez-Ramírez, A. Gallardo-Llamas, J. Phys. Chem. B 109 (2005) 20529.
[11] N.S. Ovanesyan, A.A. Shteinman, K.A. Dubkov, V.I. Sobolev, G.I. Panov, Kinet. Catal. 39 (1998) 792.
[12] K.A. Dubkov, N.S. Ovanesyan, A.A. Shteinman, E.V. Starokon, G.I. Panov, J. Catal. 207 (2002) 341.
[13] Z.X. Gao, H.S. Kim, Q. Sun, P.C. Stair, W.M.H. Sachtler, J. Phys. Chem. B 105 (2001) 6186.
[14] E.J.M. Hensen, Q. Zhu, R.A. van Santen, J. Catal. 220 (2003) 260.
[15] E. Hensen, Q.J. Zhu, P.H. Liu, K.J. Chao, R. van Santen, J. Catal. 226 (2004) 466.
[16] E.J.M. Hensen, Q. Zhu, R.A.J. Janssen, P. Magusin, P.J. Kooyman, R.A. van Santen, J. Catal. 233 (2005) 123.
[17] E.J.M. Hensen, Q. Zhu, R.A. van Santen, J. Catal. 233 (2005) 136.
[18] K.Q. Sun, H.D. Zhang, H. Xia, Y.X. Lian, Y. Li, Z.C. Feng, P.L. Ying, C. Li, Chem. Commun. (2004) 2480.
[19] K.Q. Sun, H. Xia, E. Hensen, R. van Santen, C. Li, J. Catal. 238 (2006) 186.
[20] K.Q. Sun, H.A. Xia, Z.C. Feng, R.v. Santen, E. Hensen, C. Li, J. Catal. 254 (2008) 383.
[21] J.B. Taboada, E.J.M. Hensen, I. Arends, G. Mul, A.R. Overweg, Catal. Today 110 (2005) 221.
[22] S.H. Choi, B.R. Wood, J.A. Ryder, A.T. Bell, J. Phys. Chem. B 107 (2003) 11843.
[23] N. Hansen, A. Heyden, A.T. Bell, F.J. Keill, J. Phys. Chem. C 111 (2007) 2092.
[24] P. Marturano, L. Drozdova, A. Kogelbauer, R. Prins, J. Catal. 192 (2000) 236.
[25] G.D. Pirngruber, P.K. Roy, R. Prins, Phys. Chem. Chem. Phys. 8 (2006) 3939.
[26] L. Kiwi-Minsker, D.A. Bulushev, A. Renken, J. Catal. 219 (2003) 273.
[27] G. Centi, S. Perathoner, F. Pino, R. Arrigo, G. Giordano, A. Katovic, V. Pedula, Catal. Today 110 (2005) 211.
[28] A.A. Battiston, J.H. Bitter, F.M.F. de Groot, A.R. Overweg, O. Stephan, J.A. van Bokhoven, P.J. Kooyman, C. van der Spek, G. Vanko, D.C. Koningsberger, J. Catal. 213 (2003) 251.
[29] J. Pérez-Ramírez, G. Mul, F. Kapteijn, J.A. Moulijn, A.R. Overweg, A. Doménech, A. Ribera, I. Arends, J. Catal. 207 (2002) 113.
[30] G.D. Pirngruber, P.K. Roy, R. Prins, J. Catal. 246 (2007) 147.
[31] G. Berlier, G. Ricchiardi, S. Bordiga, A. Zecchina, J. Catal. 229 (2005) 127.
[32] D. Kaucky, Z. Sobalik, M. Schwarze, A. Vondrova, B. Wichterlová, J. Catal. 238 (2006) 293.
[33] A. Heyden, B. Peters, A.T. Bell, F.J. Keil, J. Phys. Chem. B 109 (2005) 1857.
[34] A. Zecchina, M. Rivallan, G. Berlier, C. Lamberti, G. Ricchiardi, Phys. Chem. Chem. Phys. 9 (2007) 3483.
[35] H.A. Xia, K.Q. Sun, K.J. Sun, Z.C. Feng, W.X. Li, C. Li, J. Phys. Chem. C 112 (2008) 9001.
[36] E.M. El-Malki, R.A. van Santen, W.M.H. Sachtler, J. Catal. 196 (2000) 212.
[37] L.V. Pirutko, V.S. Chernyavsky, A.K. Uriarte, G.I. Panov, Appl. Catal. A 227 (2002) 143.
[38] G.I. Panov, E.V. Starokon, L.V. Pirutko, E.A. Paukshtis, V.N. Parmon, J. Catal. 254 (2008) 110.
[39] F. Kapteijn, G. Marban, J. RodriguezMirasol, J.A. Moulijn, J. Catal. 167 (1997) 256.
[40] D.M. Kurtz Jr., Chem. Rev. 90 (1990) 585.
[41] G. Centi, S. Perathoner, R. Arrigo, G. Giordano, A. Katovic, V. Pedula, Appl. Catal. A 307 (2006) 30.
[42] J. Pérez-Ramírez, M.S. Kumar, A. Brückner, J. Catal. 223 (2004) 13.
[43] J. Pérez-Ramírez, J.C. Groen, A. Brückner, M.S. Kumar, U. Bentrup, M.N. Debbagh, L.A. Villaescusa, J. Catal. 232 (2005) 318.
[44] Y. Yu, G. Xiong, C. Li, F.S. Xiao, J. Catal. 194 (2000) 487.
[45] A. Ates, A. Reitzmann, J. Catal. 235 (2005) 164.
[46] J.B. Taboada, A.R. Overweg, P.J. Kooyman, I. Arends, G. Mul, J. Catal. 231 (2005) 56.
[47] G. Carja, G. Delahay, C. Signorile, B. Coq, Chem. Commun. (2004) 1404.
[48] H.Y. Chen, W.M.H. Sachtler, Catal. Lett. 50 (1998) 125.